A SPECTROMETER SYSTEM TO STUDY PROCESSES OF THE BARYON EXCHANGE TOPOLOGY

W. F. Baker
National Accelerator Laboratory

R. M. Heinz
Indiana University

and

D. H. White
Cornell University

ABSTRACT

A high-resolution spectrometer system and its application in the study of processes topologically related to baryon exchange is discussed. The design of an experiment on backward pion-nucleon elastic scattering from 10 to 100 BeV/c is considered in detail.

INTRODUCTION

We propose an experimental layout consisting of a high-precision forward spectrometer and a recoil-particle detector to study backward meson-proton elastic scattering and other two-body final-state processes. Reactions that could be studied with this apparatus are given in Table I. Backward $\pi^{\pm}p$ elastic scattering would be studied using the apparatus as described. Category II of Table I lists experiments that could be done by rearranging the detectors and using, in some cases, some additional equipment. The beam momentum range and angular range to be investigated are listed in Table I for many reactions. Detailed studies have not been made for Category II reactions, although we shall show the feasibility of doing experiments 7-11.

All of the reactions in Table I have the common feature that, for most production angles of interest, one final-state particle leaves the target at a small laboratory angle and momentum close to that of the beam; the forward final-state particle can then be analyzed with a high-precision spectrometer. We thus envision a situation where the rather elaborate forward spectrometer would be extremely versatile for studying many reactions, while the additional equipment required to do an experiment would, in general, be tailor-made to study a specific reaction.

BEAM

A secondary beam produced at a small production angle ($\lesssim 2.5$ mrad) and with an intensity of 10^7 pions (π^+ or π^-) per burst at secondary momenta up to 100 BeV/c (for a 1/4% momentum bite) is required. The proposed 2.5 mrad secondary beam would be adequate up to 80 or 90 BeV/c. In a section of the secondary beam where the beam particles are approximately parallel, two differential Cerenkov counters, which detect K's and p's (or $\bar{p}$'s) respectively, would be located. The beam would then be focused to a 2 mm diameter spot and have a 0.5 mrad divergence. A horizontal and a vertical scintillation counter hodoscope (2 mm spatial resolution) would be located just downstream of the last beam element so that the beam particle direction can be determined with a resolution $\lesssim 0.1$ mrad. The beam hodoscopes would not usually be part of the trigger requirement because of the high beam intensity; they would be interrogated only when a trigger occurred. For $\pi^+p \rightarrow p\pi^+$ it will be necessary to have an anticoincidence on beam protons to maintain trigger selectivity in the forward spectrometer. Thus it will be necessary to limit the positive beam intensity so that there are no more than 2×10^6 protons per pulse.

APPARATUS

The experimental layout, which will be described in the context of the $\pi p \rightarrow p\pi$ experiment, is shown in Fig. 1. The apparatus will analyze recoil protons with lab angles between 1.5 and 50 mrad, while scattered π's with laboratory angles from 70° to 170° will be detected. We propose using a septum magnet (S1 in Fig. 1) to separate the beam from the scattered proton so that the proton spectrometer can be located relatively close to the H_2 target. The proton direction is measured with wire planes, with an angular resolution of 0.10 mrad, before and after the proton analyzing magnet S2. Design specifications of S1 and S2 are given in Table II. Magnet S2 would bend the protons by 60 mrad, yielding a momentum resolution of 0.25%. At 10 BeV/c the error in momentum measurement due to the multiple coulomb scattering of the proton is comparable to the inherent measurement resolution of the spectrometer. The last elements of the forward spectrometer are a scintillation counter and a threshold gas Cerenkov counter (C_p in Fig. 1) in anticoincidence. The azimuthal acceptance of the forward spectrometer is 10%.

The direction of the scattered π is measured with an array of wire spark chambers with an angular resolution of 1 mrad. In order economically to cover the pion laboratory angular range of interest, the pion wire planes are split into two sets of five planes each. A Cerenkov counter (C_π in Fig. 1), in coincidence, covers pion laboratory angles up to 90°.

TRIGGER

In the limit of 100% efficiency for C_p, only protons which have approximately the beam momentum can satisfy the forward spectrometer trigger requirement. Similarly, C_π prevents triggers from slow protons in the π arm. An array of anticoincidence counters would cover the forward 2π sr laboratory solid angle not subtended by detectors. These would be lead-scintillator sandwich counters and would drastically suppress triggers from four-prongs or final states with π^0's. An anticoincidence counter with a 1/4 cm diameter hole would be located just upstream of the H_2 target. This counter would prevent triggers from particles in the beam halo and would also be useful for focusing the beam onto the H_2 target.

The yields per hour for Type I reactions based on a 60-cm long H_2 target are given in Fig. 2. We have assumed a beam intensity of 10^7 π^- per burst, while the positive beam intensity is as close to 10^7 pions per burst as is possible without exceeding 2×10^6 protons per burst. We have used the Pb production curves of Awschalom and White (NAL report FN-191) to represent expected yields from a W target and have taken the energy dependence of the $\pi^\pm p \rightarrow p\pi^\pm$ cross section to be s^{-2}. The $\pi^+ p \rightarrow p\pi^+$ yield drops rapidly above 50 BeV/c because of the beam-intensity limitation imposed by the upper limit for the proton flux. Setting a goal of 1,000 events per momentum, we feel that the yield should be 10 events or more per hour. Figure 2 shows that these backward πp experiments as we propose them are feasible up to 80 or 90 BeV/c.

MINI OMEGA

We have looked into the improvement given by adding a magnet of modest field around the target. In the case of elastic scattering, the momentum resolution we have specified for the forward spectrometer seems quite adequate to separate π's from ρ's in the backward hemisphere, particularly when the constraint given by the pion direction is included. The question remains whether we can identify the ρ^- clearly, apart from its appearance as a bump in the forward spectrometer missing mass plot, by measuring the π^- momentum and π^0 direction. We find that it is very difficult. In Fig. 3, we have drawn a magnet of field 10 kG and one meter across. If we put detectors as shown, the sagitta will be 4 cm so that we expect a momentum accuracy of about 10-15 MeV/c, since momenta of decay products are 300-500 MeV/c. Then given that there is a missing particle, we can estimate its momentum only to about 100 MeV/c (the uncertainty in the forward spectrometer). So the ρ^- mass is uncertain to about 30%.

Let us consider doing experiments 7-11 in Category II, all of which have a forward unstable baryon. To be specific, consider

$$\pi^- + p \to N^{*o} + \rho^o \searrow \pi^+ + \pi^- .$$

Then we can require detection of both pions,and the ρ^o mass is measured directly to 5% which is very satisfactory. Now we ask if we can estimate the mass of the N^*. Assume the ρ is at 180°. Then if the mass of the N^* is m_N, the momentum of the ρ, as shown in Appendix I, is given by

$$p_\rho \approx \frac{m_p^2 - m_\rho^2}{2m_p} - \frac{m_N^2}{4p}\left(1 + \frac{m_\rho^2}{m_p^2}\right).$$

It is clear from this expression that even if Δm_ρ, Δp (p is the beam momentum) are small compared to Δp_ρ, then $\Delta (m_N^2) = 4p \times \Delta p_\rho$ which is very large even for Δp_ρ of 50 MeV/c.

So we turn to the forward spectrometer, restricting ourselves to N^* decay modes having one pion. We know that the direction of the nucleon from the N^* decay is very close to the N^* direction itself. We suppose that we measure the momentum of the N^* by momentum balance between the ρ and the beam pion. The uncertainty is dominated by the beam uncertainty, about 0.1 mrad, and momentum resolution of 0.25%. Then, if the momentum of the decay proton is p_1, the mass of the N^* is given by

$$m_N^2 \approx m_p^2 \frac{p}{p_1} + \frac{pp_1 \cdot 4 \sin^2 \frac{\theta}{2}}{1 - \frac{p_1}{p}} ,$$

where θ is the laboratory angle between the N^* and the proton, and p now refers to the N^* momentum (see Appendix II).

We also know that p_1 is between 0.70 p and p. So approximately

$$m_N^2 - m_p^2 \approx \frac{p}{\Delta p}\left(p^2 \theta^2 + m_\pi^2\right) ,$$

where $\Delta p \equiv p - p_1$.

θ is less than 2 mrad for at least 70% of the N^* (1238) decay phase space, even when p = 100 BeV/c. (If the N^* has two or more pions in its decay, the above formula is still correct if m_π is taken as the effective mass of the pions.) Then

$$\frac{\Delta\left(m_N^2 - m_p^2\right)}{\left(m_N^2 - m_p^2\right)} \approx \frac{2d\theta}{\theta} \quad ,$$

since the uncertainty in θ dominates. In fact the difference in the masses squared is measured to about 10% for the spectrometer in Fig. 1.

We conclude from this that if we wish to identify the reaction we wish to study clearly, then the backward particle (e.g. ρ, K_1^0) must be recognizable by its mass from the measurement of the charged decay. The forward baryon is identified by measuring the proton from its decay in the forward spectrometer, using those events in which the missing mass of the undetected particles is consistent with having one missing pion. (There will be a small background of events with two missing π's.) Thus we are confident that reactions 7-11 in Category II can be measured well when the backward particle and the final decay proton only are analyzed. The mini-omega magnet pays for itself handsomely.

APPENDIX I. KINEMATICS FOR FORWARD N^*.

Let
p = incident momentum
p_1 = fast forward N^* momentum
p_2 = backward particle momentum.

Then

$$p = p_1 - p_2$$

$$p + m_p = \sqrt{p_1^2 + m_1^2} + \sqrt{p_2^2 + m_2^2}$$

$$p + m_p - p_1 - \frac{m_1^2}{2p_1} \approx \sqrt{p_2^2 + m_2^2}$$

$$-p_2 + m_p - \frac{m_1^2}{2p_1} \approx \sqrt{p_2^2 + m_2^2} .$$

Square, and keep terms up to 1/p, so that

$$\not{p}_2^2 + m_p^2 - 2p_2 m_p + \frac{p_2}{p_1} m_1^2 - \frac{m_p m_1^2}{p_1} = \not{p}_2^2 + m_2^2 ,$$

p is substituted for p_1 in the following; this is accurate to $0(1/p^2)$.

$$p_2\left(2m_p - \frac{m_1^2}{p}\right) = m_p^2 - m_2^2 - \frac{m_p m_1^2}{p}$$

$$2m_p p_2 = \left[\left(m_p^2 - m_2^2\right) - \frac{m_p m_1^2}{p}\right]\left(1 + \frac{m_1^2}{2m_p p}\right)$$

$$= m_p^2 - m_2^2 - \frac{1}{p}\left[m_p m_1^2 - \left(m_p^2 - m_2^2\right)\frac{m_1^2}{2m_p}\right]$$

$$= m_p^2 - m_2^2 - \frac{1}{2m_p p}\left(2m_p^2\, m_1^2 - m_p^2\, m_1^2 + m_1^2\, m_2^2\right)$$

$$p_2 = \frac{m_p^2 - m_2^2}{2m_p} - \frac{m_1^2}{4m_p^2 p}\left(m_p^2 + m_2^2\right)$$

$$= \frac{m_p^2 - m_2^2}{2m_p} - \frac{m_1^2}{4p}\left(1 + \frac{m_2^2}{m_p^2}\right).$$

If Δm_2, Δp are small compared to Δp_2

then $$\Delta p_2 \approx -\frac{\Delta\left(m_1^2\right)}{4p}$$

or $$\Delta\left(m_1^2\right) \approx -4p\Delta p_2.$$

APPENDIX II. DECAY KINEMATICS FOR FORWARD N^*.

Let the mass of N^* be m_N, its momentum p

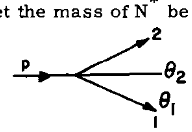

N^* decays to particles 1 and 2. Assume particle 1 is a proton and particle 2 is a pion.

From momentum conservation

$$p = p_1 \cos\theta_1 + p_2 \cos\theta_2$$

$$0 = p_1 \sin\theta_1 - p_2 \sin\theta_2.$$

Eliminate θ_2:

$$p_2^2 = p^2 + p_1^2 - 2pp_1 \cos\theta_1 .$$

From energy conservation (neglect mass of particle 2, and assume $m_p << p_1$, $m_N << p$).

$$\sqrt{p^2 + m_N^2} = \sqrt{p_2^2 + m_2^2} + p_1 + \frac{m_p^2}{2p_1}$$

$$\sqrt{p_2^2 + m_2^2} = p + \frac{m_N^2}{2p} - p_1 - \frac{m_p^2}{2p_1} .$$

Square and retain terms 0(o).

$$p_2^2 + m_2^2 = p^2 + p_1^2 + m_N^2 - 2pp_1 - m_p^2 \frac{p}{p_1} - m_N^2 \frac{p_1}{p} + m_p^2$$

$$m_N^2 \left(1 - \frac{p_1}{p}\right) = 2pp_1 (1 - \cos\theta) - m_p^2 \left(1 - \frac{p}{p_1}\right) + m_2^2$$

$$\left(\frac{m_N^2}{p} - \frac{m_p^2}{p_1}\right) (p - p_1) = 2pp_1 (1 - \cos\theta) + m_2^2 .$$

We remember that $p_1 \approx p$, and θ is small:

$$m_N^2 - m_p^2 = \frac{p}{\Delta p} (p^2\theta^2 + m_2^2).$$

Table I. Reactions.

Reaction	Beam Momentum	Angular Range
I. $\pi^{\pm}p \to p\pi^{\pm}$	10-100 BeV/c[a]	$0 \gtrsim u \gtrsim -1.0\ (\text{BeV/c})^2$
II.		
1. $\bar{p}p \to \pi^+\pi^-$		
2. $\bar{p}p \to K^+K^-$		
3. $\bar{p}p \to \bar{p}p$		
4. $\pi^{\pm}p \to \pi^{\pm}p$ polarization		
5. $\pi^{\pm}p \to \pi^{\pm}p$		$t < -1\ (\text{BeV/c})^2$
6. $pp \to pp$		$t < -1\ (\text{BeV/c})^2$
7. $\pi^{\pm}p \to \pi^{\pm}N^{*+}$, $\hookrightarrow p\pi^o$		u small
8. $pp \to pN^{*+}$	up to 100 BeV/c	t small
9. $\pi^-p \to \rho^oN^{*o}$, $\hookrightarrow p\pi^-$		
10. $\pi^{\pm}p \to K^+Y^{*\pm}$		u small
11. $\pi^{\pm}p \to K^+\Sigma^{\pm}$		u small
12. $\pi^-p \to p\rho^-$, $\hookrightarrow \pi^-\pi^o$		
13. $K^+p \to pK^+$	10-30 BeV/c	u small

[a] To cover the angular range of interest between 10 and 20 BeV/c, it will be necessary to do the experiment with the forward spectrometer in two positions, covering 1.5 - 50 mrad and 40 - 90 mrad respectively.

Table II. Magnet Specifications.

Magnet	S1	S2	Mini Omega
Maximum Field	17 kG	20 kG	20 kG
Length	4 m	10 m	1.3 m
Maximum Bend for 100 BeV/c	10 mrad	60 mrad	-
Septum Thickness	1/4 cm	20 cm	-
Aperture Height	1.0 cm	1.0 m	0.5 m
Aperture Width	3.0 cm	2.0 m	1.3 m
Cost	~ $50 K	~ $2 M[a]	$75 K[b]

[a]The downstream analyzing magnet, S2, is a bulky and expensive item. Advantages may be gained by subdividing it into several smaller units with successively increasing aperture. This solution would not only improve the portability; but, by removal of one or more units, it would also permit larger acceptances at lower momenta where less bending power is needed. The specific way of subdividing, the question of normal versus superconducting coils, and the magnetic field strength are economic as well as technical questions and are beyond the scope of this report.

[b]This is a 48D48 presently in use at Brookhaven.

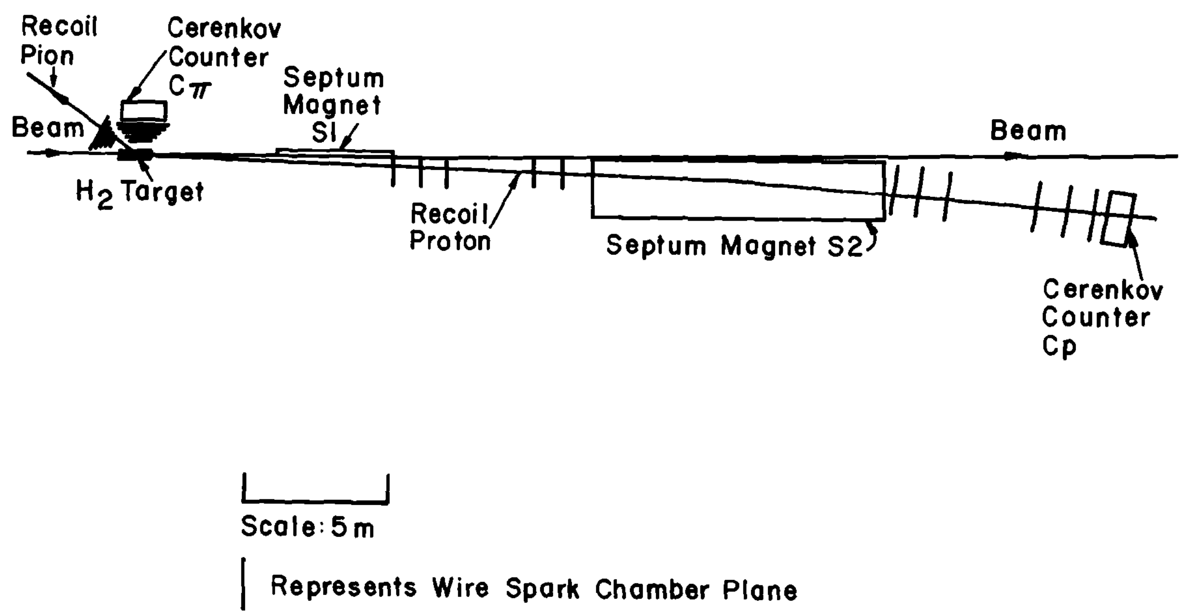

Fig. 1. The experimental layout.

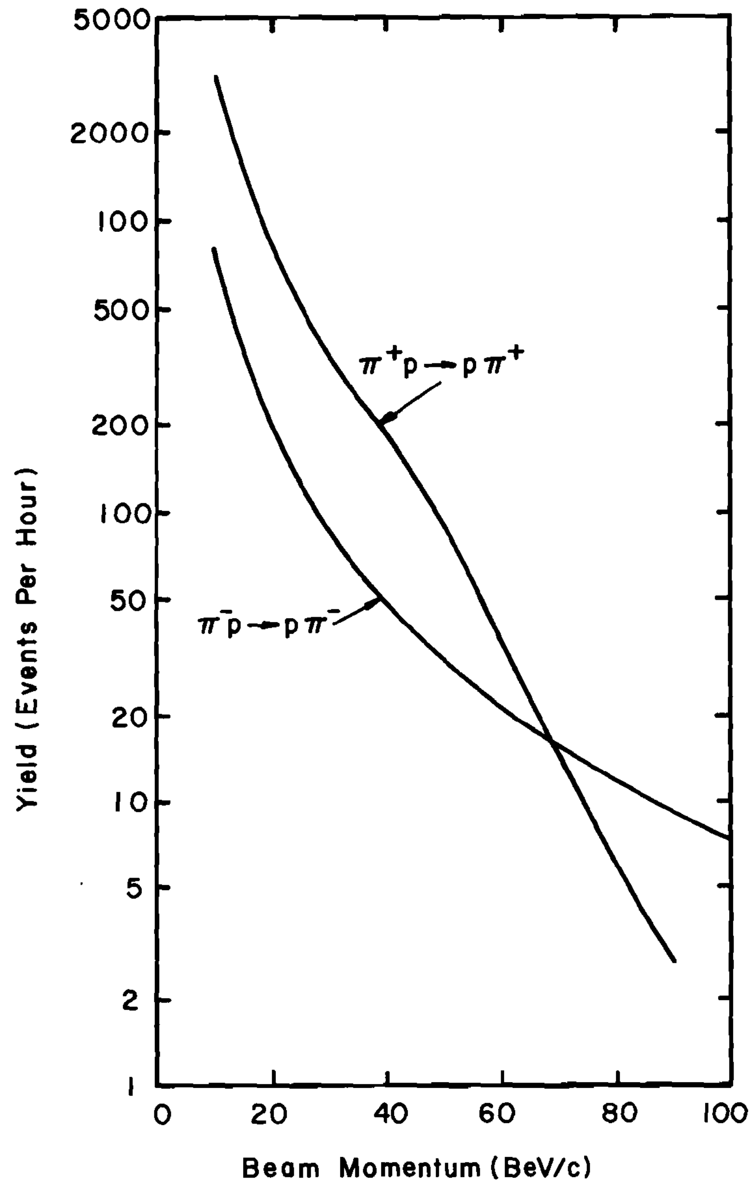

Fig. 2. Yields for $\pi^- p \to p\pi^-$ and $\pi^+ p \to p\pi^+$.

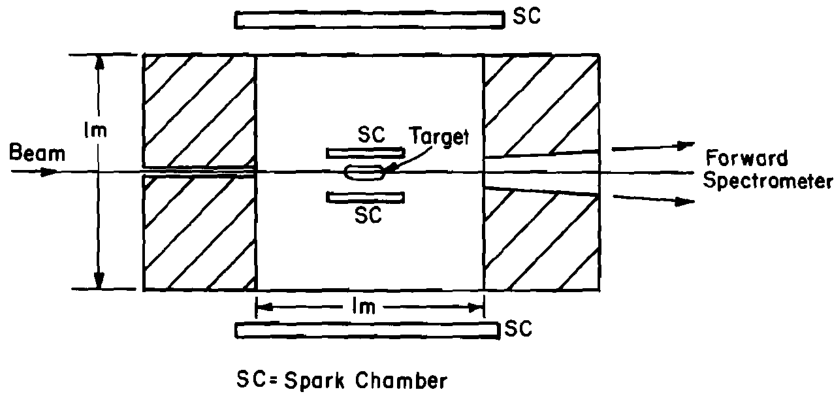

Fig. 3. Mini Omega experimental layout.